Cell. Mol. Life Sci. (2010) 67:3725–3737
DOI 10.1007/s00018-010-0401-z

Cellular and Molecular Life Sciences

RESEARCH ARTICLE

Calcineurin activity is required for the completion of cytokinesis

Megan Chircop · Chandra S. Malladi · Audrey T. Lian · Scott L. Page · Michael Zavortink · Christopher P. Gordon · Adam McCluskey · Phillip J. Robinson

Received: 20 September 2009 / Revised: 8 April 2010 / Accepted: 4 May 2010 / Published online: 23 May 2010
© Springer Basel AG 2010

Abstract Successful completion of cytokinesis requires the spatio-temporal regulation of protein phosphorylation and the coordinated activity of protein kinases and phosphatases. Many mitotic protein kinases are well characterized while mitotic phosphatases are largely unknown. Here, we show that the Ca^{2+}- and calmodulin-dependent phosphatase, calcineurin (CaN), is required for cytokinesis in mammalian cells, functioning specifically at the abscission stage. CaN inhibitors induce multinucleation in HeLa cells and prolong the time cells spend connected via an extended intracellular bridge. Upon Ca^{2+} influx during cytokinesis, CaN is activated, targeting a set of proteins for dephosphorylation, including dynamin II (dynII). At the intracellular bridge, phospho-dynII and CaN are co-localized to dual flanking midbody rings (FMRs) that reside on either side of the central midbody ring. CaN activity and disassembly of the FMRs coincide with abscission. Thus, CaN activity at the midbody plays a key role in regulating the completion of cytokinesis in mammalian cells.

Keywords Calcineurin · Cytokinesis · Dephosphorylation · Dynamin II

Introduction

Cytokinesis is the final stage of cell division that generates two separate daughter cells. Cytokinesis failure of somatic cells results in aneuploidy, which leads to genomic instability and thus contributes to the initiation and progression of tumorigenesis. Cytokinesis in animal cells requires three steps: (1) membrane ingression, (2) vesicle trafficking, and (3) membrane abscission [1]. Membrane ingression begins during anaphase and requires the assembly and activity of the actin-myosin II contractile ring and the septin ring proteins [1]. The membrane is fully constricted by the end of telophase, whereby the anti-parallel microtubules forming the mitotic spindle and associated proteins are compressed to form an intracellular bridge between nascent daughter cells. At the center of the bridge is the midbody, consisting of several proteins [2], such as γ-tubulin [3], centriolin [4], and the exocyst complex [5]. They assemble into a single ring structure, called the midbody ring (MR) [5]. The MR is not contractile and is unable to account for abscission on its own. It appears to act as a recruitment scaffold for the abscission machinery, which itself remains to be identified. Vesicle trafficking is a major hallmark of the middle stage of cytokinesis, with vesicle fusion occurring adjacent to the MR. This stage is relatively slow and there are no gross cellular morphology changes at the midbody. In contrast, the final stage, membrane abscission, is a very rapid event that results in final formation of independent daughter cells. This suggests the presence of a triggering mechanism. Almost nothing is known about the molecular mechanisms of abscission itself. After

Electronic supplementary material The online version of this article (doi:10.1007/s00018-010-0401-z) contains supplementary material, which is available to authorized users.

M. Chircop (✉) · C. S. Malladi · A. T. Lian · S. L. Page · M. Zavortink · P. J. Robinson
Children's Medical Research Institute,
The University of Sydney, 214 Hawkesbury Road,
Westmead, NSW 2145, Australia
e-mail: mchircop@cmri.com.au

C. P. Gordon · A. McCluskey
Chemistry, School of Environmental and Life Sciences,
The University of Newcastle, Callaghan, NSW 2308, Australia

abscission, the MR may be inherited by one of the daughter cells [5].

In lower organisms, protein phosphatases play different roles in mitosis. In *Saccharomyces cerevisiae* [6, 7] and *Schizosaccharomyces pombe* [8, 9], mitotic exit and coordination of cytokinesis are driven by the dual serine-threonine and tyrosine-protein phosphatase, Cdc14 (Flp1). A large number of proteins are phosphorylated upon mitotic entry [10] and a significant proportion of these are mediated by Cdk, which drives mitotic progression. Thus the action of Cdc14 is, in part, to counteract Cdk activity by dephosphorylating Cdk substrates [11]. Most Cdc14 substrates identified to date are dephosphorylated during anaphase. Very few substrates during telophase and cytokinesis are known. The phosphatase(s) that acts to reverse Cdk phosphorylation during mitotic exit in eukaryotes is not well understood. Homologues of Cdc14 exist in most if not all eukaryotes, but they do not seem to have the same central function in late mitosis as in budding yeast [12]. In *Caenorhabditis elegans*, depletion of CeCDC-14 by RNAi causes defects in cytokinesis, however, this is most likely due to a failure to form an intact central spindle [13]. The human genome encodes two Cdcl4 homologues, hCdc14A and hCdc14B. Their roles are poorly understood. However, hCdc14A has been linked to centrosome separation and cytokinesis [14, 15], while hCdc14B participates in centrosome duplication and microtubule stabilization [16]. In most eukaryotes, Cdc14 is dispensable for mitotic exit, indicating that other phosphatases are required to complete cytokinesis.

CaN (or PP2B) is a serine-threonine phosphatase that exists as a heterodimer composed of a 58 to 64-kDa catalytic subunit (A subunit; PP2B-A) and a 19-kDa Ca^{2+} regulatory subunit (B subunit; PP2B-B). It is a Ca^{2+}/calmodulin-activated enzyme involved in the regulation of a variety of cellular functions [17]. The requirement for CaN in mammalian cytokinesis has not yet been reported. CaN has been linked to cytokinesis in *S. pombe* [18, 19]. It is upregulated during exit of *Xenopus* oocytes from metaphase of meiosis II [20, 21]. Ca^{2+} influx is essential for completion of cytokinesis in *Drosophila* spermatocytes [22] and localized Ca^{2+} influx is commonly observed to accompany cytokinesis in other cells [23]. In mammalian cells, Ca^{2+} signaling during cytokinesis is thought to be essential in triggering the synchronous and coordinated fusion with the plasma membrane of endosomal membranes stored inside cells [24]. For example, a rise in intracellular Ca^{2+} triggers rapid fusion of late endosomes and lysosomes with the plasma membrane [25]. Inhibition of calmodulin activity blocks regression of the centriole from the intracellular bridge to the cell center, thus cytokinesis is repressed and the two daughter cells remain connected via a long intracellular bridge [26]. In neurons, CaN is responsible for dephosphorylating a group of proteins, called the dephosphins, many of which are cdk5 substrates, to trigger synaptic vesicle endocytosis [27]. The non-neuronal isoforms of four of these dephosphins: Eps15, epsin, amphiphysin II and dynamin II, are mitotically phosphorylated and/or have been implicated in mitosis in mammalian cells [28–31]. In this study, we show that CaN is required for cytokinesis in mammalian cells and its activity is specifically associated with the late abscission stage.

Materials and methods

Chemical synthesis of RO-3306

RO-3306 was synthesized in-house (Fig. 1) by a method modified from that previously reported [32]. To a suspension of thiophen-2-yl-methylamine (0.226 g, 2 mmol) and rhodanine (2-thio-4-thiazolin-4-one) (0.133 g, 1 mmol) in acetonitrile (5 ml) was added trubutylamine (107 ml, 0.45 mmol) at room temperature (25°C). The mixture was stirred for 5 min and resulted in a clear solution, at this point the solution was cooled to between 0 and 5°C in an ice-water bath. To this, mercuric chloride (0.272 g, 1 mmol) was added portion-wise (three portions) over a 30-min period. After complete addition, the mixture was stirred at room temperature (22–27°C) for 2 days. The solids were removed by filtration through a Celite plug. The Celite was then washed successively with dichloromethane (15 ml), and methanol (20 ml). The combined solvents were removed in vacuo and the crude residue taken up in ethyl acetate (10 ml) and water (10 ml). The layers were separated and the aqueous layer was extracted with dichloromethane (2 × 10 ml). The organic layers were combined, dried over $MgSO_4$, and the solvent removed in vacuo to afford an off-white solid. Recrystallization from acetonitrile yielded 0.135 g, 63% of 2-[(thiopen-2-ylmethyl)-amido]-thiazol-4-one as a white solid. To a suspension of 2-[(thiopen-2-ylmethyl)-amido]-thiazol-4-one (above) (92 mg, 0.43 mmol) and quinoline-6-carbaldehyde (82 mg, 0.52 mmol) in toluene (5 ml) were added benzoic acid (5.3 mg, 0.043 mmol) and piperidine (4.37 ml, 0.44 mmol) at room temperature. The mixture was refluxed for 16 h, cooled, and the precipitate, 5-(quinolin-6-ylmeth-(*Z*)-ylidine)-2-[(thiophen-2-ylmethyl)-amino]-thiazol-4-one collected, 25 mg, 17%.

Cell culture, cell synchronization, and drug treatment

HeLa cervical carcinoma and HCT116 colon carcinoma cells were maintained in RPMI 1640 medium supplemented with 10% fetal bovine serum (FBS) and grown at

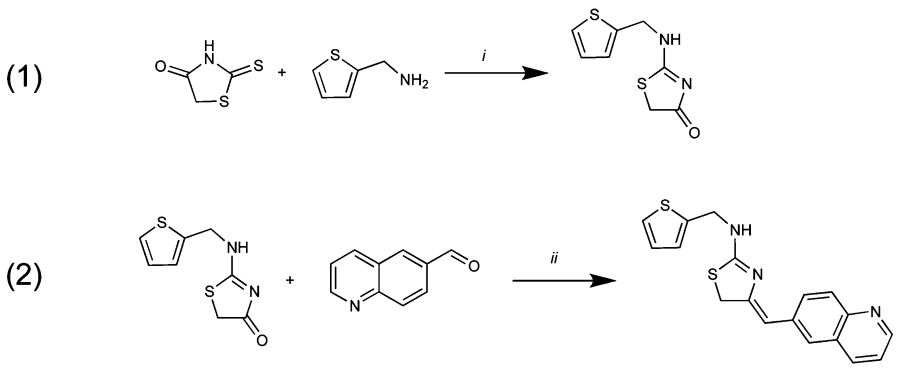

Reagents and Conditions. (i) $HgCl_2$, DIEA; (ii) Piperidine, $PhCO_2H$

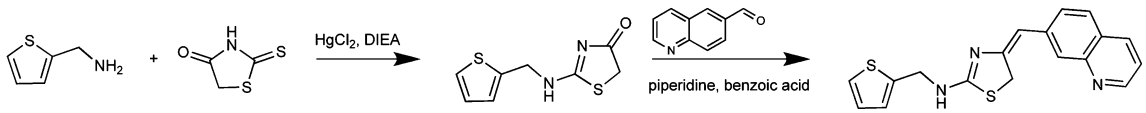

Fig. 1 Synthesis of RO-3306

37°C in a humidified 5% CO_2 atmosphere. Cells grown on coverslips were synchronized at the G_1/S border by double thymidine block. Cells were then released into the cell cycle following thymidine wash-out. At 8-h post-release, cells were treated with EGTA (Sigma) for 10 h then fixed for immunofluorescence microscopy analysis. For mitotic synchronization, cells were treated with 0.5 μg/ml nocodazole for 16 h. Mitotic arrested cells were collected by "mitotic shake-off". When required, they were washed three times with pre-warmed medium, then seeded into 10-cm^2 dishes and incubated at 37°C/5% CO_2 to allow progression through mitosis. Cells were collected at the indicated time post-release from nocodazole for immunoblot analysis. Alternatively, cells were synchronized at the G_2/M border by treatment with the selective cdk1 small-molecule inhibitor, RO-3306 (9 μM) for at least 18 h. Cells were allowed to progress through mitosis following RO-3306 wash-out. Where indicated, cells were treated with either 30 μM CsA, 100 μM CaN-11R-AID peptide (Calbiochem; [33] or 1 mM EGTA at either 0, 1.5, or 2 h post-release and incubated at 37°C/5% CO_2 for the indicated period of time.

Time-lapse microscopy analysis

Immediately following release into the cell cycle following synchronization with RO-3306, cells were viewed with an Olympus IX80 inverted microscope and a time-lapse series was acquired using a fully motorized stage, 10× objective, and Metamorph software using the Time-lapse modules. Temperature control was achieved using the Incubator XL, providing a humidified atmosphere with 5% CO_2. Imaging was performed for 20 h with a lapse time of 5 or 10 min. Where indicated, EGTA (1 mM) or CsA (50 μM) were added at the indicated time following RO-3306 wash-out.

Immunofluorescence and confocal microscopy

Cells were fixed in ice-cold 100% methanol for 10 min at −20°C and then blocked in 3% bovine serum albumin/PBS for 45 min before the required primary antibody was applied. The following antibodies were used: anti-CaN (AB-1; Calbiochem), anti-dynI phospho-S778 [34], anti-actin (Sigma), anti-α-tubulin (clone DM1A; Sigma) and anti-γ-tubulin (GTU88; Sigma). Fluorescein- or Texas Red dye-conjugated AffiniPure secondary antibodies (Jackson ImmunoResearch Laboratories, Inc.) were then applied. Cell nuclei were counterstained with DAPI (4′, 6′-diamidino-2-phenylindole; Sigma). Cells were washed three times with PBS between each step except for after-blocking. Cells were viewed and scored with a fluorescence microscope (Ziess). Fluorescence images were captured and processed using a Lieca DMIRB/E confocal microscope. Alternatively, images were captured under an Olympus IX80 inverted microscope using 40× or 100× oil immersion lenses and deconvolved using AutoDeblur v9.3 (AutoQuant Imaging, Watervliet, NY). XZ and YX images were reconstructed using Metamorph software.

Immunoblotting

Cellular extracts were prepared by incubating cells in ice-cold lysis buffer [25 mM Tris–HCl pH 7.4, 150 mM NaCl, 1 mM EDTA, 1 mM EGTA, 1 mM PMSF, 1% Triton X-100, and EDTA-free Complete protease inhibitor cocktail (Roche)] and the supernatant was collected following centrifugation at 13,000 rpm for 30 min at 4°C. GST-amphiphysin II (amphII)-SH3 domain fusion protein was expressed in *Escherichia coli* and purified using glutathione-Sepharose beads (Amersham Biosciences) according to the manufacturer's instructions. DynII protein was enriched by incubating the cellular extracts with purified GST-amphII-SH3 domain bound to glutathione-Sepharose beads for 1 h at 4°C. Beads were washed extensively with ice-cold lysis buffer. Bound proteins were fractionated by SDS-PAGE for immunoblot analysis. The following antibodies were used: anti-dynII (C-18, Santa Cruz Biotechnology), anti-dynI, anti-dynI phospho-S774 and anti-dynI phospho-S778 [34], anti-α-tubulin (clone DM1A; Sigma), anti-γ-tubulin (GTU88; Sigma) and anti-CaN (AB-1; Calbiochem). Antibody bound to the indicated protein was detected by incubation with a horseradish peroxidase-conjugated secondary antibody (Sigma). Blotted proteins were visualized using the ECL detection system (Pierce).

In vitro CaN phosphatase assays

Total rat brain extract was prepared [34] and lysates were prepared from HeLa cells synchronized in mitosis. These lysates were mixed with GST-amphII-SH3 beads to enrich for dynI and dynII, respectively. In vitro CaN phosphatase assays were performed as described previously [27] with minor modifications using equalized amounts of dynI and dynII as substrate. In brief, dynI and dynII bound to GST-amphII-SH3 beads were incubated in 30 µl of 10 mM Tris–HCl (pH 7.4) containing 10 mM NaCl, 200 nM calmodulin, 200 µM Ca^{2+}, and 1 mM Mn^{2+}. Where indicated, 1 µg of purified CaN (4 units/reaction) was added. Samples were incubated at 30°C for various time intervals. The reaction was terminated by freezing on dry ice.

Results

CaN localizes to flanking midbody rings and is required for the abscission stage of cytokinesis

The *ppb1*$^{+}$ gene encoding, a fission yeast *S. pombe* homologue of the catalytic subunit of mammalian CaN, is essential for yeast cytokinesis [18]. Therefore, we asked whether CaN activity is required for mammalian cytokinesis by using time-lapse analysis (Fig. 2a). HeLa cells were synchronized with RO-3306, a selective small-molecule inhibitor of cdk1 that reversibly arrests human cells at the G_2/M border of the cell cycle and allows for effective cell synchronization in early mitosis [32]. Following RO-3306 wash-out, HeLa cells treated with the CaN inhibitor, CsA, rounded-up as they entered mitosis and progressed from prophase to metaphase (Pro-Met) and metaphase to full membrane ingression (Met-Ing) with similar kinetics to untreated control cells (Fig. 2b). Thus, a role for CaN in chromosome alignment, chromosome segregation and the first stage of cytokinesis, furrow ingression, is excluded. In contrast, time-lapse analysis revealed that CsA-treated cells fail cytokinesis and that the point of failure was the abscission stage. This was evident since these cells remained connected via an intracellular bridge for a prolonged period of time prior to either generation of a multinucleated cell or two independent cells (Ing-comp or multi; Fig. 2b). No cytokinesis defects were observed in untreated control cells (Fig. 2b). The intracellular bridge length was substantially longer in CsA-treated cells [Fig. 2c; 3.95 ± 0.21 µm ($n = 42$) for control cells vs. 7.43 ± 0.59 µm ($n = 35$) for cells treated with CsA for 6 h], indicating bridge persistence, but an inability to complete abscission. Similarly, prolonged exposure of cells to CsA resulted in an increase in the number of cells connected via an intracellular bridge and in the number of multinucleated cells (Fig. 2d). At the longest time point analyzed after CsA treatment (8 h), abscission was aborted, resulting in two independent daughter cells or multinucleated cells (Fig. 2d). Two additional CaN antagonists that utilize distinct CaN inhibitory mechanisms, FK506 and the inhibitory peptide CaN-11R-AID [33], also increased multinucleation (data not shown), suggesting the effect is specifically mediated by CaN rather than off-target actions of these compounds. CsA treatment also caused an increase in the percentage of multinucleates in the HCT116 colon cancer cell line (Fig. 2e), suggesting that CaN activity during cytokinesis may be a general requirement of different cell types. Thus, the abscission stage of cytokinesis requires CaN activity in these two cell lines.

We next sought to determine the localization of CaN during cytokinesis. At the onset of cytokinesis (anaphase) and during the ingression phase of cytokinesis (telophase), we found CaN diffusely localizing to the cytoplasm and a small amount accumulated to the midzone (Fig. 3a). CaN did not co-localize with actin (Fig. 3a), indicating that it is not associated with the cleavage furrow or contractile ring. During the abscission stage of cytokinesis we found that it is specifically localized to the midbody region (Fig. 3a). Midzone and midbody localization was not disrupted by CsA treatment, suggesting that CaN activity is not specifically required for its recruitment to these locations

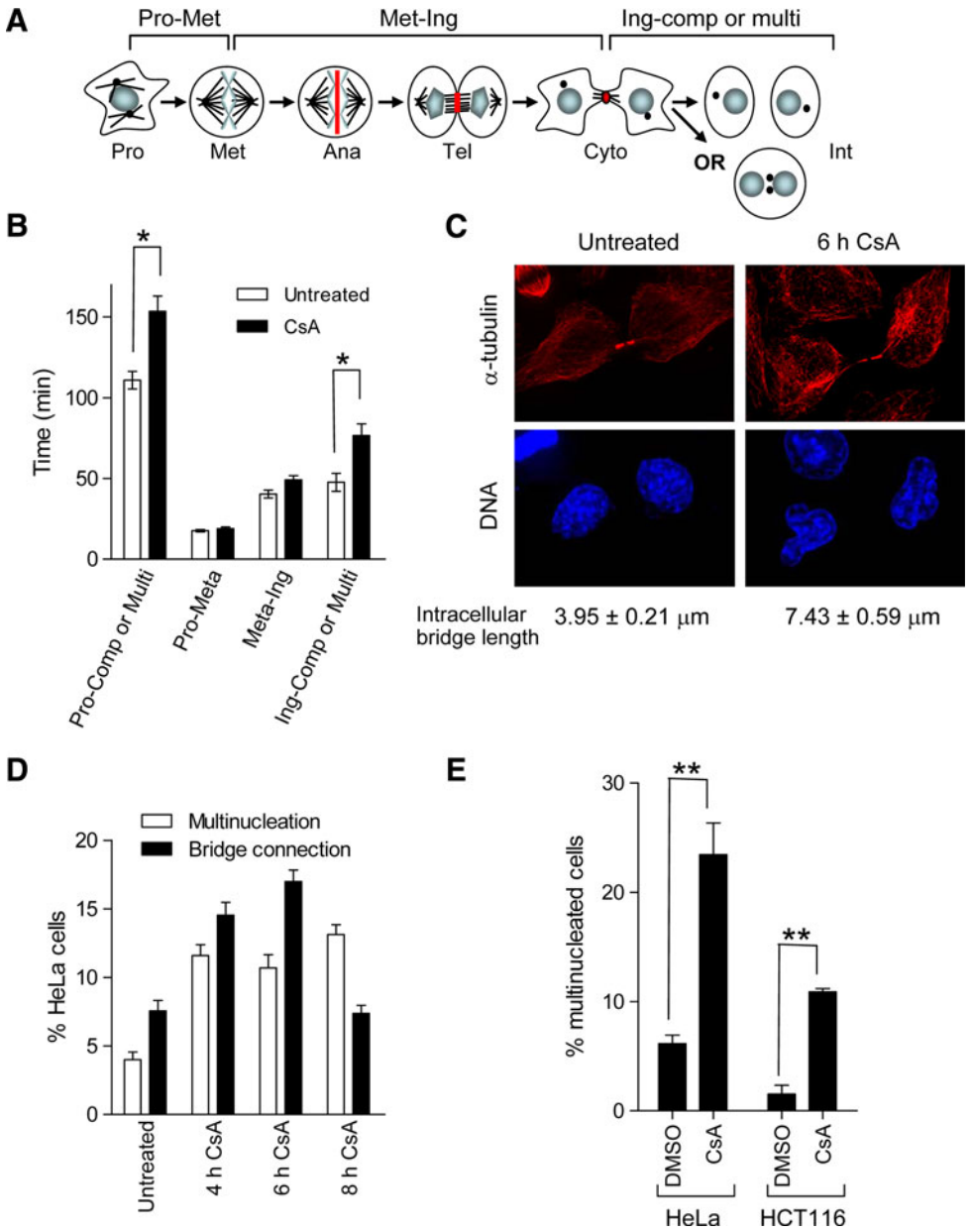

Fig. 2 CaN participates in the abscission phase of cytokinesis. **a** Schematic diagram of the phases in mitosis. *Pro* prophase, *Met* metaphase, *Ana* anaphase, *Tel* telophase, *Cyto* cytokinesis, *Int* interphase. Shown above is the mitotic process divided into three sections, which were the time intervals calculated for time-lapse analysis. (1) Pro to Met, (2) Met to completion of membrane ingression (Ing), (3) Ing to either generation of two independent daughter cells (Comp) or formation of a multinucleated cell (Multi). **b** HeLa cells were synchronized using RO-3306, and then visualized by time-lapse microscopy. The CaN inhibitor, CsA (30 μM), was added to the cells 1.5 h after RO-3306 washout; i.e., specifically at the time when cells were entering cytokinesis. Cells were scored ($n > 120$ cells per sample) for the time taken to undergo mitosis as described in **a**. The graph shows that CaN inhibition by CsA prolongs the overall time cells spend in mitosis. Specifically, following completion of membrane ingression, the abscission stage is prolonged. *Statistically significant, $p < 0.05$, Student's t test. **c** Representative immunofluorescence microscopy of cells treated with CsA (30 μM) for 6 h, demonstrating that inhibition of CaN with CsA extends the length of the intracellular bridge and prevents abscission ($n = 35$). The lower panel shows nuclear DAPI staining to indicate cell position. **d** Asynchronously growing HeLa cells were treated in the presence or absence of CsA (30 μM) for the indicated period of time. Cells were subsequently stained for α-tubulin, then analyzed by immunofluorescence microscopy to quantify the number of multinucleated cells and the number of cells that were connected by an intracellular bridge. The graphs show the mean ± SEM from three independent experiments. **e** HeLa and HCT116 cells were synchronized using RO-3306. Following RO-3306 washout, cells were treated with the CaN inhibitor, CsA (30 μM), and vehicle (0.1% DMSO) for 6 h, then fixed, stained for α-tubulin, and scored for the number of multinucleated cells. The graphs show the mean ± SD from two independent experiments and reveals that inhibition of CaN induces multinucleation in both cell lines. **Statistical significance $p < 0.01$

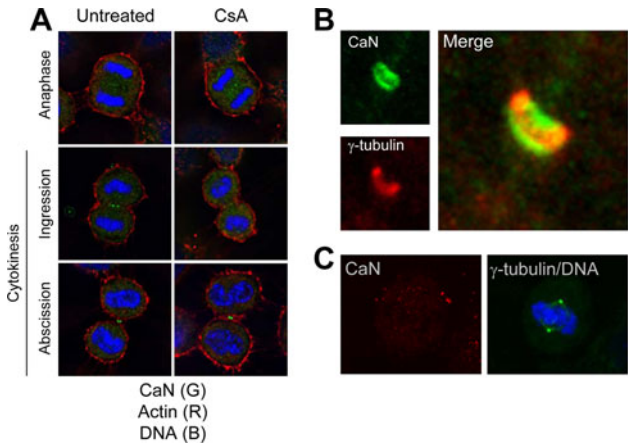

Fig. 3 CaN localizes to dual "flanking midbody rings" (FMRs). **a** CaN localizes to the midbody. Asynchronously growing HeLa cells were treated in the presence or absence of CsA (30 μM) for 6 h then stained with antibodies for actin and CaN. Representative immunofluorescence microscopy images of cells in anaphase, and in cytokinesis during the ingression (telophase) and abscission stages. Images demonstrate that CaN localizes to the cytoplasm and midzone during the ingression stage of cytokinesis and then to the midbody during the abscission stage of cytokinesis even in an inactive state (CsA-treated). **b** Representative microscopy images of the intracellular bridge region reveal that CaN localizes to regions on either side of the central γ-tubulin MR, termed FMRs. **c** A representative image of a HeLa cell in metaphase showing the centrosomes stained for γ-tubulin. Co-staining for CaN reveals that it does not locate to the mitotic centrosomes. DNA is shown in *blue*

(Fig. 3a). Since abscission is known to occur on one side of the γ-tubulin MR [5], we used deconvolution microscopy of the intracellular bridge to determine if CaN co-localized with γ-tubulin. To our surprise, CaN was not present in the MR but was exclusively localized to twin rings that flank the central γ-tubulin MR (Fig. 3b). Since abscission is known to occur on one side of the γ-tubulin MR [5], we have called these "flanking midbody rings" (FMRs). This localization was highly specific as we did not observe CaN localizing to any other discrete structures throughout mitosis, such as the mitotic centrosomes (Fig. 3c). After abscission, the MR is found in the daughter cell opposite the abscission site (data not shown; [5]). However, we find that the FMRs are no longer present in this structure, suggesting their disassembly during or immediately after abscission.

Calcium triggers abscission in HeLa cells

CaN is a Ca^{2+}-dependent phosphatase, suggesting that Ca^{2+} plays an upstream role for CaN in cytokinesis in mammalian cells. Previous studies support a role for Ca^{2+} in the later stages of mitosis but not specifically to cytokinesis [22–24]. The role of Ca^{2+} in cytokinesis has been incompletely characterized due to its multifunctional cellular roles and its association with different mitotic stages apart from cytokinesis. To dissect apart the multiple roles Ca^{2+} plays during mitosis, we observed live cells using time-lapse microscopy following addition of the Ca^{2+} chelator, EGTA, at specific times during mitotic progression: (1) immediately upon release from RO-3306 wash-out, when cells were entering mitosis, and (2) at 1.5 h following RO-3306 wash-out, when cells had completed anaphase and were entering cytokinesis. Under the first condition, we observed a block in mitotic progression at anaphase with the cleavage furrow ingressed by approximately 50% (Movie S1), as previously observed [35]. Under the second condition, the post-anaphase addition of EGTA produced a cytokinesis failure phenotype indistinguishable from that of CsA treatment. EGTA-treated cells entered cytokinesis but were unable to complete it, resulting in an increase in binucleated cells (Fig. 4a, b). Time-lapse microscopy analysis revealed that these cells took twice as long to complete mitosis (successfully or not) than control cells and the time delay was determined to be due to failure in the abscission stage of cytokinesis (Fig. 4c). Details of this finding are highlighted in several representative time-lapse movies (Movie S2-4). In control cells, ingression requires 15–20 min, but abscission is an extremely rapid step in mitosis, such that the intracellular bridge is cut soon after its formation (Movie S2). After normal ingression, EGTA-treated cells showed a massive delay in abscission and the intracellular bridge persisted for prolonged periods of time. In some cases, the intracellular bridge did not lengthen and the cleavage furrow eventually regressed, producing a binucleated cell (Movie S3). In other cases, the intracellular bridge extended to extremely long lengths, which appeared to "snap" (Movie S4). In an independent approach, cells were synchronized at the G_1/S transition by double thymidine block then treated with EGTA upon mitotic entry. Blocking Ca^{2+} influx this way also caused cytokinesis failure (Fig. 4d). Collectively, these data indicate that Ca^{2+} plays two distinct roles during mitosis at anaphase and at abscission. A role for Ca^{2+} in abscission has not previously been demonstrated.

DynII is a calcineurin substrate during cytokinesis

In the brain, dynI is one of the highest affinity substrates for CaN yet identified [27]. The dephosphorylation of dynI at S774 and S778 is required for the rapid triggering of synaptic vesicle endocytosis in neurons [36]. We have recently discovered that the ubiquitously expressed dynamin isoform, dynII, is phosphorylated at S764 specifically during mitosis (unpublished data). We now show that S764 is phosphorylated throughout mitosis and is dephosphorylated at the time of cytokinesis (at 3 h after release from nocodazole block; Fig. 5a). The specificity of the phospho-Ser antibody for dynII was confirmed by showing that

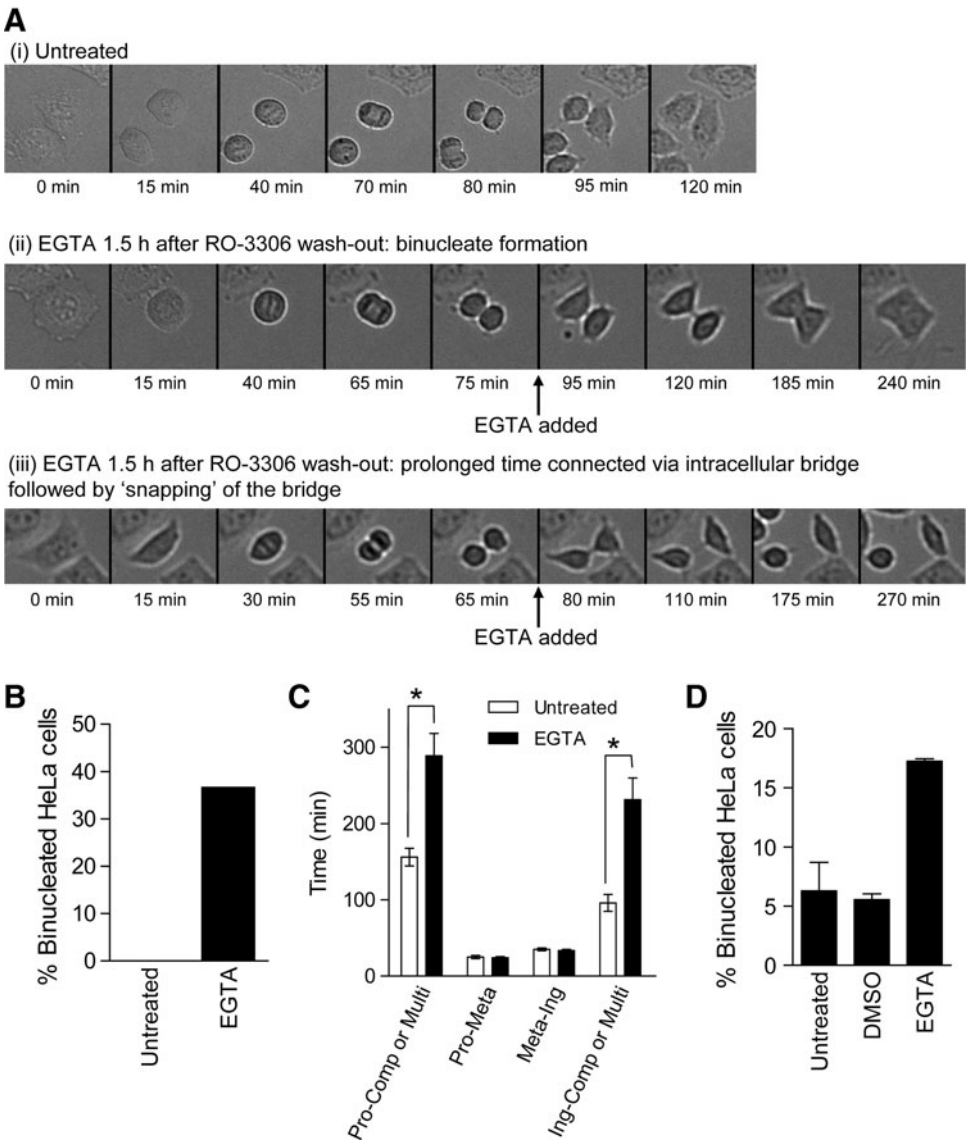

Fig. 4 Ca^{2+} chelation blocks cytokinesis at the abscission step. **a** Selected frames from representative time-lapse movies of (*i*) an untreated HeLa cell and (*ii*, *iii*) HeLa cells treated with EGTA (1 mM) at 1.5 h following RO-3306 wash-out. **b**, **c** HeLa cells were synchronized at the G_2/M transition by the cdk1 inhibitor, RO-3306, and then visualized by time-lapse microscopy. At 1.5 h post-release (anaphase), cells were treated with EGTA. Following mitosis, cells were scored for multinucleation, a marker of cytokinesis failure. The graph illustrates that EGTA treatment induces multinucleation (**b**). Cells were also scored for the time taken to reach a critical mitotic step. The graph illustrates that EGTA prolongs the mitotic phase compared to untreated controls. Specifically, following completion of chromosome segregation and membrane ingression, the abscission stage is prolonged. This occurs in cells that complete mitosis successfully, generating two mononucleated cells and unsuccessfully, generating a binucleated cell (**c**). *Statistically significant, $p < 0.05$, Student's *t* test. **d** HeLa cells were synchronized at the G_1/S transition by double-thymidine block. At 8 h post-release from thymidine block, cells were treated with EGTA for 10 h. The graph displays the mean ± SEM from three independent experiments and shows that EGTA causes multinucleation

mutation of the S764 to alanine abolishes detection of ectopically expressed GFP-dynII-PRD in mitotically synchronized HeLa cell lysates (Fig. 5b). Therefore, we asked whether dynII is also an in vivo CaN substrate during cytokinesis. The ability of CaN to dephosphorylate dynII during cytokinesis was assessed in vivo. The specific small-molecule CaN inhibitors, CsA and FK506, prevented dynII dephosphorylation at S764 for at least 4 h following release from nocodazole block (Fig. 5a). If the addition of CsA was delayed for 2 h after nocodazole release, the dephosphorylation was blocked as effectively as if added immediately upon release (Fig. 5c). The findings indicate that CaN is activated specifically at a late stage in cytokinesis and just prior to abscission.

We confirmed that dynII-S764 is a direct target of CaN by performing an in vitro assay. A pool of dynII mitotically

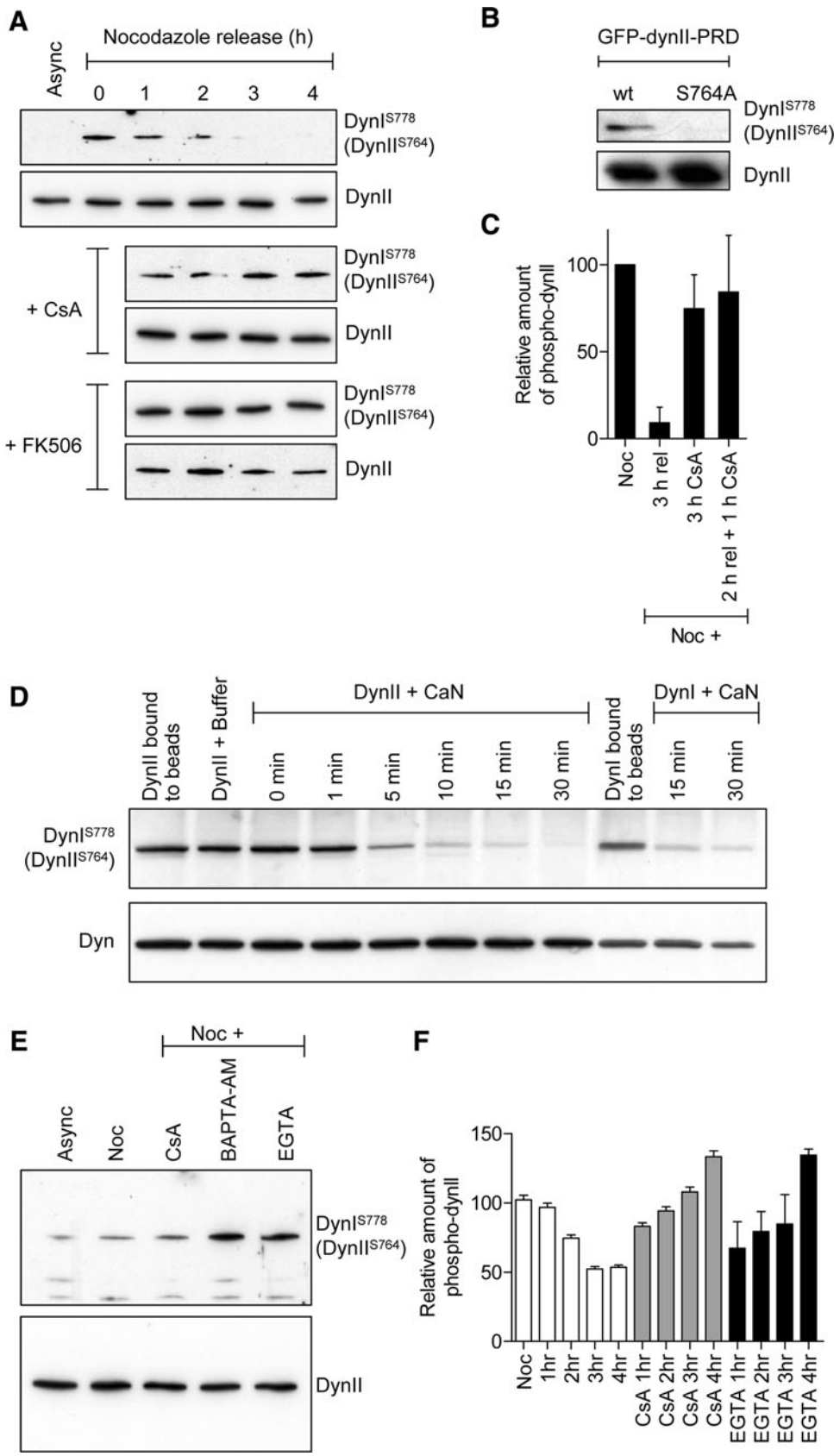
A
Nocodazole release (h)
Async
0
1
2
3
4
DynI^S778 (DynII^S764)
DynII
+ CsA
+ FK506
B
GFP-dynII-PRD
wt
S764A
C
Relative amount of phospho-dynII
100
50
0
Noc
3 h rel
3 h CsA
2 h rel + 1 h CsA
Noc +
D
DynII bound to beads
DynII + Buffer
DynII + CaN
0 min
1 min
5 min
10 min
15 min
30 min
DynI bound to beads
DynI + CaN
15 min
30 min
Dyn
E
Noc +
Async
Noc
CsA
BAPTA-AM
EGTA
F
Relative amount of phospho-dynII
150
100
50
0
Noc
1hr
2hr
3hr
4hr
CsA 1hr
CsA 2hr
CsA 3hr
CsA 4hr
EGTA 1hr
EGTA 2hr
EGTA 3hr
EGTA 4hr

◀ **Fig. 5** Calcineurin dephosphorylates dynII during cytokinesis. **a** HeLa cells were blocked in prometaphase using nocodazole and were subsequently released into either drug-free medium or medium containing the CaN inhibitor, CsA or FK506 (30 μM). Cells were collected and lysates were prepared at the indicated times following release. Following GST-amphII-SH3 pull-down, samples were immunoblotted to assess the phosphorylation status of dynII and to determine dynII levels. Results are representative of at least two independent experiments. **b** HeLa cells ectopically expressing wt or phospho-deficient (S764A) GFP-dynII-PRD were synchronized in mitosis with nocodazole. The prepared lysates were immunoblotted for phospho-dynII using the phospho-dynI-S778 antibody and dynII levels using a GFP antibody. **c** Reduction in phospho-dynII observed 3 h following release from nocodazole block is prevented by treatment with CsA equally as efficient when it is added at the time of release or at 2 h post-release. A graph illustrating the quantitation of phospho-dynII in the indicated conditions presented as a densitometric ratio normalized to the amount of phospho-dynII in mitotic synchronized HeLa cells (Noc). Results are mean ± SEM, $n \geq 3$. **d** In vitro CaN phosphatase assay. Purified dynI purified from sheep brain and purified dynII from HeLa cells synchronized in mitosis were incubated in the presence or absence of purified CaN for the indicated period of time. An immunoblot revealed rapid dephosphorylation of dynII at S764, occurred as efficiently as dynI at S778 (the homologous amino acid), and that dephosphorylation increased with incubation time. **e** HeLa cells were blocked in prometaphase using nocodazole and subsequently released into drug-free medium for 2 h. Cells were then treated with the CaN inhibitor, CsA, or the calcium chelators BAPTA-AM and EGTA for 1 h. Cellular extracts were prepared and immunoblotted following GST-amphII-SH3 pull-down to assess the phosphorylation status of dynII at S764 and total dynII levels. **f** HeLa cells were blocked in prometaphase using nocodazole and subsequently released into drug-free medium, or in the presence of the CaN inhibitor, CsA, or the calcium chelator, EGTA, for the indicated period of time. Reduction in phospho-dynII over time following release from nocodazole block is prevented by treatment with CsA and EGTA. Graph (mean ± SD) illustrates the quantitation of phospho-dynII in the indicated conditions presented as a densitometric ratio normalized to the amount of phospho-dynII in mitotic synchronized HeLa cells (Noc). $n = 2$

phosphorylated on S764 was purified from mitotically synchronized HeLa cells, while phospho-dynI was purified from rat brain as a positive control. CaN efficiently dephosphorylated S764 in dynII in a Ca^{2+}- and calmodulin-dependent manner (Fig. 5d). Notably >90% of dynII was dephosphorylated within 5 min (Fig. 5d). Under the same conditions, CaN efficiently dephosphorylated dynI at S778; >90% dephosphorylation occurred within 15 min (Fig. 5d), as we reported previously [27].

Since CaN is a Ca^{2+}-dependent phosphatase, the data suggest that abscission may be controlled by a burst of Ca^{2+} influx at the midbody leading to dynII dephosphorylation. DynII dephosphorylation was monitored during cytokinesis in the presence of two types of Ca^{2+} chelators. Excess EGTA in the media 2 h after nocodazole release prevented dynII dephosphorylation on S764 by blocking Ca^{2+} influx at the time of abscission (Fig. 5e). EGTA not only prevented cytokinesis-induced dynII dephosphorylation but also induced further increases in phosphorylation (Fig. 5f). This pattern of dynII phosphorylation is analogous to treatment with the CaN inhibitor, CsA (Fig. 5f), suggesting that Ca^{2+} influx at the midbody activates CaN. To determine whether Ca^{2+} had an intracellular target such as CaN, we used the membrane-permeable Ca^{2+} chelator, BAPTA-AM. BAPTA-AM also prevented dynII dephosphorylation and induced further increases in phosphorylation in cells undergoing cytokinesis (Fig. 5e). Thus, Ca^{2+} influx is required for the activation of CaN during cytokinesis, suggesting that Ca^{2+} is essential for abscission and that CaN is a major target.

Phospho-dynII co-localizes with CaN at the FMRs

Previous reports have observed dynII in the general midbody region [2, 37, 38]. Our data now shows that this dynII is primarily in the phosphorylated form. In an analogous manner to CaN, phospho-dynII was not broadly distributed throughout the intracellular bridge, nor was it present in the centrally located MR, but was exclusively localized to twin rings that flank the central MR (Fig. 6a). Dual staining revealed that phospho-dynII co-localizes with CaN at the FMRs (Fig. 6b). The ring organization of the MR was confirmed by three-dimensional reconstruction of a z-series of a HeLa cell undergoing cytokinesis stained with γ-tubulin (Movie S5). Unlike the single larger MR (1.62 ± 0.1 μm diameter), phospho-dynII was specifically localized to two smaller rings (1.12 ± 0.05 μm diameter; Fig. 6a). XZ and YZ sections were reconstructed from a z-series of high-resolution microscopy images of phospho-dynII. The YZ plane-of-view confirmed the presence of phospho-dynII in two FMRs. The XZ plane showed that phospho-dynII is absent from the central part of these sites, revealing that it is present in twin ring structures (Fig. 6c). Thus, the intracellular bridge consists of a single large central γ-tubulin MR, flanked by two smaller FMRs.

The findings above show that CaN localization to the FMRs is not disrupted by its inhibitor, CsA (Fig. 3a). Immunofluorescence microscopy analysis reveals that phospho-dynII also remains at the FMRs following inhibition of CaN activity by either CsA or CaN-11R-AID (Fig. 6d). Thus CaN activity is not required for its recruitment to the FMRs. The Ca^{2+} chelator EGTA also had no effect on the FMR localization of phospho-dynII and CaN (Fig. 6e). We confirmed that after abscission the MR is found in one of the two daughter cells (data not shown and [5]). However, these remnant MRs lack either phospho-dynII- or CaN-labeled FMRs (data not shown). This suggests that the FMRs may be disassembled during or immediately after abscission.

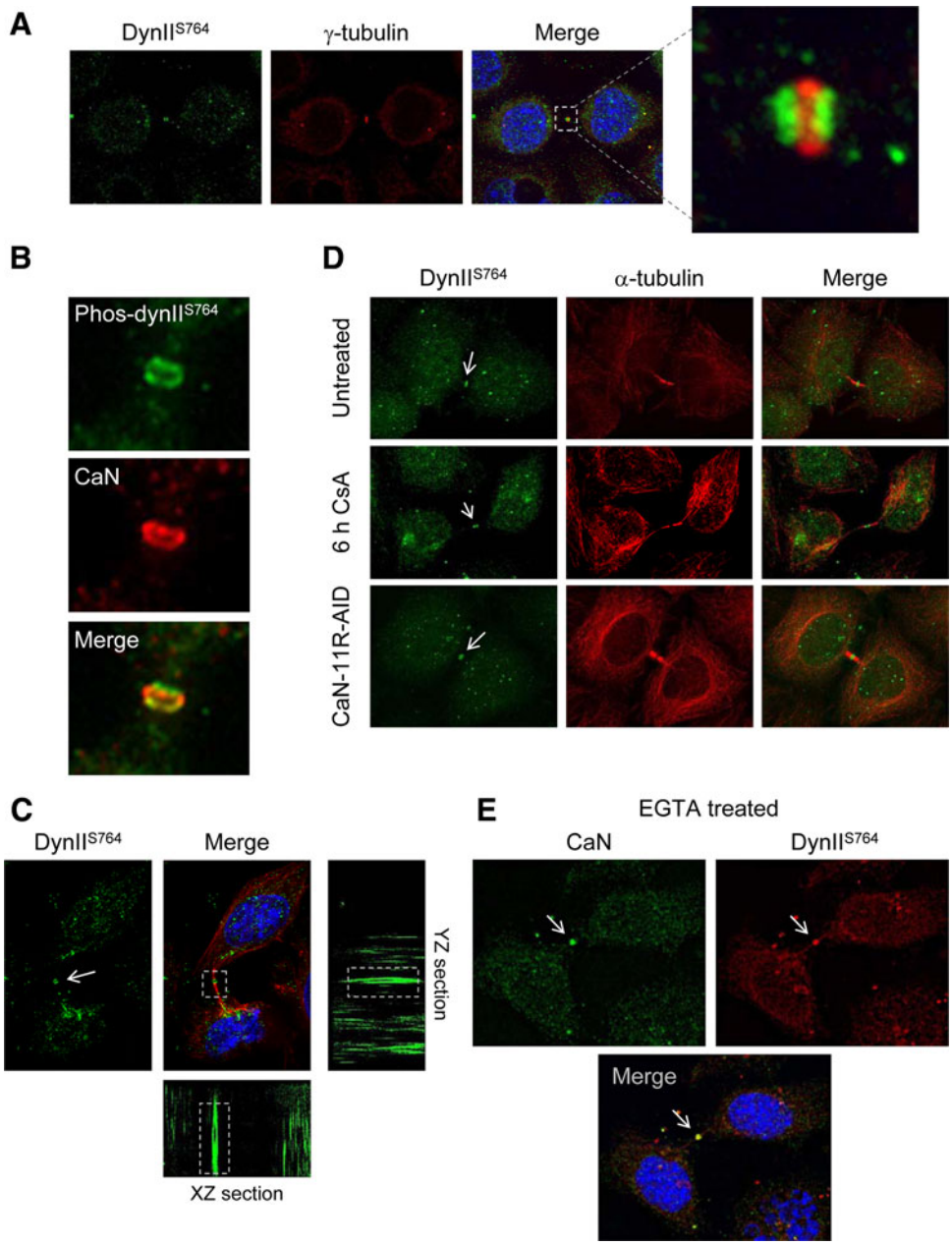

Fig. 6 Phospho-dynII co-localizes with CaN at FMRs. **a** Asynchronously growing HeLa cells were stained for endogenous phospho-dynII-S764 (*green*) and γ-tubulin (*red*). Representative deconvolved microscopy images demonstrating that phospho-dynII-S764 resides in two distinct FMR regions of the intracellular bridge that flank the central MR composed of γ-tubulin. **b** A representative image of the intracellular bridge region of an asynchronously growing HeLa cell showing phospho-dynII (*green*) and CaN (*red*) co-localizing at the FMRs. **c** Phospho-dynII assembles into two rings at the midbody—FMRs. Representative deconvolved images of a HeLa cell undergoing cytokinesis stained for α-tubulin and phospho-dynII. *XZ* and *YZ* planes-of-view were reconstructed from a z-series of images revealing that phospho-dynII is present in two rings at the intracellular bridge. **d** HeLa cells were treated for 6 h with CsA or synchronized at the G_1/S transition by double-thymidine block and then treated in with the CaN inhibitory peptide, CaN-11R-AID. Cells were subsequently stained for phospho-dynII-S764 (*green*) and α-tubulin (*red*). Representative immunofluorescence microscopy images reveal that phospho-dynII localization at the FMRs is not disrupted by inhibition of CaN. **e** A representative immunofluorescence image of a HeLa cell in cytokinesis showing phospho-dynII and CaN co-localizing at FMRs in the presence of the Ca^{2+} chelator, EGTA (1 mM). HeLa cells were fixed, stained, and analyzed 3 h following release from RO-3306 block. EGTA was added at 2 h after RO-3306 washout

Discussion

We demonstrate that the Ca^{2+}- and calmodulin-dependent phosphatase, CaN, is required for cytokinesis in mammalian cells, extending a previous report of a role for CaN in yeast cytokinesis [18]. Our major additional finding is that it specifically functions during the abscission phase, essentially leading to completion of cytokinesis. Functional

inhibition of CaN resulted in cells spending a prolonged period of time connected via an intracellular bridge and an increase in multinucleated cells. During cytokinesis, the activation of CaN by Ca^{2+} resulted in dephosphorylation of a set of substrate proteins and we reveal that the endocytic protein, dynII, is one such substrate. CaN-mediated dephosphorylation of this group of proteins, exemplified by dephosphorylation of dynII, coincides with completion of abscission to generate two independent daughter cells. This suggests that CaN activity is required for cellular abscission rather than for earlier events of cytokinesis. Our observations raise the possibility that abscission is a rapid CaN-triggered process.

We reveal that CaN localizes to a specific sub-compartment within the intracellular bridge during the abscission stage of cytokinesis. This sub-compartment comprises dual FMRs facing a single central MR at the intracellular bridge. FMRs contain phospho-dynII and CaN and most likely other molecular components. Neither phospho-dynII nor CaN localized to the ingressing furrow, indicating that they may be directly recruited to the midbody, assembling at FMRs late in mitosis. This three-ring structure persists until the phosphatase CaN is activated. The MR is a known structural template for recruitment of key cytokinesis players like centriolin and the exocyst complex [5]. In addition, it may play a role in recruiting/anchoring proteins to the FMR. The abscission stage therefore involves a three-ring system—a single large γ-tubulin MR flanked by two smaller rings composed of (at least) phospho-dynII and CaN. As previously reported [5], we also observe the MR persisting in one of the two daughter cells after cytokinesis completion, but no detectable FMRs, either as dynII, phospho-dynII, or CaN. Thus, the FMRs are more transient structures that appear to disassemble prior to or during abscission and this may be induced in-part by CaN-mediated protein dephosphorylation. The identification of other FMR components is likely to provide further insight into the underlying mechanisms of abscission.

Our findings indicate that CaN activation is one of the last molecular events found to occur prior to abscission. In support of this idea, we were unable to detect dynII antibody-labeled FMRs without corresponding phospho-dynII FMR labeling (data not shown). Moreover, CaN activity was specifically required for the abscission stage and had no detectable role in any earlier cytokinesis steps. Thus, abscission itself must be a rapid event and therefore we propose that CaN activation must be temporally regulated to ensure that cytokinesis does not occur prematurely.

Centriole movement towards the cell center coincides with CaN activation at the FMRs. The mother centriole transiently moves to the intracellular bridge during cytokinesis and its departure from this location back to the cell center has previously been associated with the timing of cellular abscission [39]. The CaN activator, calmodulin (CaM), localizes to the intracellular bridge during cytokinesis in HeLa cells [40–42] and its functional inhibition produces a comparable cytokinesis failure phenotype to CaN inhibition in Dictyostelium [43] and HeLa cells [42]. Cytokinesis failure induced by CaM inhibition has been associated with a block in centriole movement from the intracellular bridge to the cell center in PtK2 cells [26]. It will be important to determine if CaN inhibition also blocks centriole movement from the intracellular bridge. Thus, one possibility is that only when CaM and CaN are activated would the centriole return to the cell center, subsequently allowing abscission to occur. This raises the possibility that CaN substrates may be delivered to the intracellular bridge as centrosome cargo.

The endocytic protein, dynII, was previously linked to cytokinesis in a variety of species and more recently was associated with the abscission stage of cytokinesis in mammalian cells [31]. Endocytosis has been linked to cytokinesis in plants [44] and this link has recently begun to emerge in mammalian cells [24, 45, 46]. However, it is unclear if dynII functions during cytokinesis in an endocytic-dependent or -independent manner. Here, we reveal that dynII is dephosphorylated at the time of cytokinesis, suggesting that this may be involved in its cytokinesis function. Dephosphorylation may stimulate dynII GTPase activity or may promote its interaction with a specific binding protein. It will be important to determine whether dynII phosphorylation affects binding of proteins like syndapin II and/or other endocytic proteins [34, 47, 48]. Overall, our findings reveal a new molecular pathway that involves the protein phosphatase CaN, whose activity results in the dephosphorylation of a group of cellular proteins, such as dynII, and this is associated with cellular abscission.

Acknowledgments We wish to thank Sandra L. Schmid for providing the *Baculovirus* purified dynII protein. Charlotte M. Smith, Maggie Ma, Annie Quan, and Anna Powell are thanked for their technical assistance. We thank Patrick Tam and Roger Reddel for critical reading of the manuscript. This work was supported by grants from the National Health and Medical Research Council (NH&MRC) of Australia (PJR) and the NH&MRC Peter Doherty Fellowship (MC).

References

1. Glotzer M (2005) The molecular requirements for cytokinesis. Science 307:1735–1739
2. Skop AR, Liu H, Yates J 3rd, Meyer BJ, Heald R (2004) Dissection of the mammalian midbody proteome reveals conserved cytokinesis mechanisms. Science 305:61–66
3. Julian M, Tollon Y, Lajoie-Mazenc I, Moisand A, Mazarguil H, Puget A, Wright M (1993) gamma-Tubulin participates in the

formation of the midbody during cytokinesis in mammalian cells. J Cell Sci 105(Pt 1):145–156
4. Gromley A, Jurczyk A, Sillibourne J, Halilovic E, Mogensen M, Groisman I, Blomberg M, Doxsey S (2003) A novel human protein of the maternal centriole is required for the final stages of cytokinesis and entry into S phase. J Cell Biol 161:535–545
5. Gromley A, Yeaman C, Rosa J, Redick S, Chen CT, Mirabelle S, Guha M, Sillibourne J, Doxsey SJ (2005) Centriolin anchoring of exocyst and SNARE complexes at the midbody is required for secretory-vesicle-mediated abscission. Cell 123:75–87
6. Shou W, Seol JH, Shevchenko A, Baskerville C, Moazed D, Chen ZW, Jang J, Charbonneau H, Deshaies RJ (1999) Exit from mitosis is triggered by Tem1-dependent release of the protein phosphatase Cdc14 from nucleolar RENT complex. Cell 97:233–244
7. Visintin R, Hwang ES, Amon A (1999) Cfi1 prevents premature exit from mitosis by anchoring Cdc14 phosphatase in the nucleolus. Nature 398:818–823
8. Cueille N, Salimova E, Esteban V, Blanco M, Moreno S, Bueno A, Simanis V (2001) Flp1, a fission yeast orthologue of the *S. cerevisiae* CDC14 gene, is not required for cyclin degradation or rum1p stabilisation at the end of mitosis. J Cell Sci 114:2649–2664
9. Trautmann S, Wolfe BA, Jorgensen P, Tyers M, Gould KL, McCollum D (2001) Fission yeast Clp1p phosphatase regulates G2/M transition and coordination of cytokinesis with cell cycle progression. Curr Biol 11:931–940
10. Dephoure N, Zhou C, Villen J, Beausoleil SA, Bakalarski CE, Elledge SJ, Gygi SP (2008) A quantitative atlas of mitotic phosphorylation. Proc Natl Acad Sci USA 105:10762–10767
11. Visintin R, Craig K, Hwang ES, Prinz S, Tyers M, Amon A (1998) The phosphatase Cdc14 triggers mitotic exit by reversal of Cdk-dependent phosphorylation. Mol Cell 2:709–718
12. Trautmann S, McCollum D (2002) Cell cycle: new functions for Cdc14 family phosphatases. Curr Biol 12:R733–R735
13. Gruneberg U, Glotzer M, Gartner A, Nigg EA (2002) The CeCDC-14 phosphatase is required for cytokinesis in the *Caenorhabditis elegans* embryo. J Cell Biol 158:901–914
14. Kaiser BK, Zimmerman ZA, Charbonneau H, Jackson PK (2002) Disruption of centrosome structure, chromosome segregation, and cytokinesis by misexpression of human Cdc14A phosphatase. Mol Biol Cell 13:2289–2300
15. Yuan K, Hu H, Guo Z, Fu G, Shaw AP, Hu R, Yao X (2007) Phospho-regulation of HsCdc14A by polo-like kinase 1 is essential for mitotic progression. J Biol Chem 282:27414–27423
16. Cho HP, Liu Y, Gomez M, Dunlap J, Tyers M, Wang Y (2005) The dual-specificity phosphatase CDC14B bundles and stabilizes microtubules. Mol Cell Biol 25:4541–4551
17. Shibasaki F, Hallin U, Uchino H (2002) Calcineurin as a multifunctional regulator. J Biochem 131:1–15
18. Yoshida T, Toda T, Yanagida M (1994) A calcineurin-like gene ppb1(+) in fission yeast—mutant defects in cytokinesis, cell polarity, mating and spindle pole body positioning. J Cell Sci 107:1725–1735
19. Zhang YJ, Sugiura R, Lu YB, Asami M, Maeda T, Itoh T, Takenawa T, Shuntoh H, Kuno T (2000) Phosphatidylinositol 4-phosphate 5-kinase its3 and calcineurin Ppb1 coordinately regulate cytokinesis in fission yeast. J Biol Chem 275:35600–35606
20. Mochida S, Hunt T (2007) Calcineurin is required to release *Xenopus* egg extracts from meiotic M phase. Nature 449:336–340
21. Nishiyama T, Yoshizaki N, Kishimoto T, Ohsumi K (2007) Transient activation of calcineurin is essential to initiate embryonic development in *Xenopus laevis*. Nature 449:341–345
22. Wong R, Hadjiyanni I, Wei HC, Polevoy G, McBride R, Sem KP, Brill JA (2005) PIP2 hydrolysis and calcium release are required for cytokinesis in Drosophila spermatocytes. Curr Biol 15:1401–1406
23. Groigno L, Whitaker M (1998) An anaphase calcium signal controls chromosome disjunction in early sea urchin embryos. Cell 92:193–204
24. Boucrot E, Kirchhausen T (2007) Endosomal recycling controls plasma membrane area during mitosis. Proc Natl Acad Sci USA 104:7939–7944
25. McNeil PL, Kirchhausen T (2005) An emergency response team for membrane repair. Nat Rev Mol Cell Biol 6:499–505
26. Yu YY, Dai G, Pan FY, Chen J, Li CJ (2005) Calmodulin regulates the post-anaphase reposition of centrioles during cytokinesis. Cell Res 15:548–552
27. Liu JP, Sim ATR, Robinson PJ (1994) Calcineurin inhibition of dynamin-I GTPase activity coupled to nerve-terminal depolarization. Science 265:970–973
28. Chen H, Slepnev VI, Di Fiore PP, De Camilli P (1999) The interaction of epsin and Eps15 with the clathrin adaptor AP-2 is inhibited by mitotic phosphorylation and enhanced by stimulation-dependent dephosphorylation in nerve terminals. J Biol Chem 274:3257–3260
29. Floyd SR, Porro EB, Slepnev VI, Ochoa GC, Tsai LH, De Camilli P (2001) Amphiphysin 1 binds the cyclin-dependent kinase (cdk) 5 regulatory subunit p35 and is phosphorylated by cdk5 and cdc2. J Biol Chem 276:8104–8110
30. Kariya K, Koyama S, Nakashima S, Oshiro T, Morinaka K, Kikuchi A (2000) Regulation of complex formation of POB1/epsin/adaptor protein complex 2 by mitotic phosphorylation. J Biol Chem 275:18399–18406
31. Liu YW, Surka MC, Schroeter T, Lukiyanchuk V, Schmid SL (2008) Isoform and splice-variant specific functions of dynamin-2 revealed by analysis of conditional knock-out cells. Mol Biol Cell 19:5347–5359
32. Vassilev LT, Tovar C, Chen SQ, Knezevic D, Zhao XL, Sun HM, Heimbrook DC, Chen L (2006) Selective small-molecule inhibitor reveals critical mitotic functions of human CDK1. Proc Natl Acad Sci USA 103:10660–10665
33. Terada H, Matsushita M, Lu YF, Shirai T, Li ST, Tomizawa K, Moriwaki A, Nishio S, Date I, Ohmoto T, Matsui H (2003) Inhibition of excitatory neuronal cell death by cell-permeable calcineurin autoinhibitory peptide. J Neurochem 87:1145–1151
34. Anggono V, Smillie KJ, Graham ME, Valova VA, Cousin MA, Robinson PJ (2006) Syndapin I is the phosphorylation-regulated dynamin I partner in synaptic vesicle endocytosis. Nat Neurosci 9:752–760
35. Tombes RM, Borisy GG (1989) Intracellular free calcium and mitosis in mammalian cells: anaphase onset is calcium modulated, but is not triggered by a brief transient. J Cell Biol 109:627–636
36. Tan TC, Valova VA, Malladi CS, Graham ME, Berven LA, Jupp OJ, Hansra G, McClure SJ, Sarcevic B, Boadle RA, Larsen MR, Cousin MA, Robinson PJ (2003) Cdk5 is essential for synaptic vesicle endocytosis. Nat Cell Biol 5:701–710
37. Thompson HM, Skop AR, McNiven MA (2002) Dynamin is a component of the intercellular bridge and is required for cytokinesis in hepatocytes. Hepatology 36:212A
38. Thompson HM, Skop AR, Euteneuer U, Meyer BJ, McNiven MA (2002) The large GTPase dynamin associates with the spindle midzone and is required for cytokinesis. Curr Biol 12:2111–2117
39. Piel M, Nordberg J, Euteneuer U, Bornens M (2001) Centrosome-dependent exit of cytokinesis in animal cells. Science 291:1550–1553
40. Li CJ, Heim R, Lu P, Pu Y, Tsien RY, Chang DC (1999) Dynamic redistribution of calmodulin in HeLa cells during cell division as revealed by a GFP-calmodulin fusion protein technique. J Cell Sci 112(Pt 10):1567–1577
41. Torok K, Wilding M, Groigno L, Patel R, Whitaker M (1998) Imaging the spatial dynamics of calmodulin activation during mitosis. Curr Biol 8:692–699

42. Yu YY, Dai G, Chen J, Wen CJ, Zhao DH, Li CJ (2003) The distribution of calmodulin with midbody and its involvement in cytokinesis regulation. Shi Yan Sheng Wu Xue Bao 36:335–341
43. Liu T, Williams JG, Clarke M (1992) Inducible expression of calmodulin antisense RNA in Dictyostelium cells inhibits the completion of cytokinesis. Mol Biol Cell 3:1403–1413
44. Jurgens G (2005) Cytokinesis in higher plants. Annu Rev Plant Biol 56:281–299
45. Schweitzer JK, Burke EE, Goodson HV, D'Souza-Schorey C (2005) Endocytosis resumes during late mitosis and is required for cytokinesis. J Biol Chem 280:41628–41635
46. Warner AK, Keen JH, Wang YL (2006) Dynamics of membrane clathrin-coated structures during cytokinesis. Traffic 7:205–215
47. Chen Y, Deng L, Maeno-Hikichi Y, Lai M, Chang S, Chen G, Zhang JF (2003) Formation of an endophilin-Ca^{2+} channel complex is critical for clathrin-mediated synaptic vesicle endocytosis. Cell 115:37–48
48. Qualmann B, Kelly RB (2000) Syndapin isoforms participate in receptor-mediated endocytosis and actin organization. J Cell Biol 148:1047–1062